

Origin of quasi-constant pre-exponential factors for adatom diffusion on Cu and Ag surfaces

Handan Yildirim, Abdelkader Kara, and Talat S. Rahman

Department of Physics, University of Central Florida, Orlando, Florida 32816-2385, USA

(Received 20 June 2007; revised manuscript received 1 September 2007; published 18 October 2007)

Many-body interaction potentials from the embedded atom method with two functionals and electronic structure calculations based on density functional theory and the plane-wave pseudopotential method are used to calculate the pre-exponential factors for self-diffusion of adatoms via hopping on Cu(100) and Ag(100) surfaces with and without steps. The pre-exponential factors are found to be in the range of 10^{-3} cm²/s for all investigated processes regardless of whether substrate vibrational dynamics are included or omitted. When substrate dynamics are ignored, compensation effects between stiffening and softening of the vibrational frequencies of the diffusing atom are responsible for this quasi-constant pre-exponential. When these dynamics are included, subtle cancellations in the vibrational free energy make the local contribution of the diffusing atom the dominant one.

DOI: [10.1103/PhysRevB.76.165421](https://doi.org/10.1103/PhysRevB.76.165421)

PACS number(s): 68.35.Md, 68.35.Fx, 66.30.Fq, 63.22.+m

I. INTRODUCTION

Thermally activated processes often control the end product in technologically important processes such as thin film growth and heterogeneous catalysis. Detailed and accurate knowledge of relevant energetics and dynamics of such processes is thus essential if simulation of spatio-temporal evolution of materials is to have predictive power. One of the major computational techniques used to study such evolution of materials is kinetic Monte Carlo calculating diffusion coefficients estimated from harmonic transition state theory.^{1,2} These coefficients depend on two main ingredients, namely, the activation energy barrier and the pre-exponential factor (or prefactor). Much attention has been given to the calculation of the activation energies, while the prefactor is often assumed to take the “standard value” of 10^{-3} cm²/s.³⁻⁸ It is also customary to note that uncertainties in the activation energies would generate fluctuations in the diffusion coefficient that are much larger than those generated by deviations in the prefactors from the standard value. Since accurate determination of the activation energies (for example, using density functional theory) is becoming more and more feasible, focus has been turning toward a more realistic determination of the prefactors. Such knowledge is certainly important for cases in which accurately determined energy barriers for competing processes lie very close in value to one another.

In previous publications,⁹⁻¹¹ a detailed description of a quantum mechanical approach to calculate these prefactors within the harmonic/quasiharmonic approximation has been presented and recently applied to the case of adatoms hopping on terraces and steps of Cu(100) and Cu(110).⁹ Indeed, the prefactor was found to be of the order of 10^{-3} cm²/s with a variation of about less than 1 order of magnitude. We should note here that a full quantum mechanical treatment of the prefactor is not a trivial matter even when the interatomic interaction potential is of a semi-empirical nature.⁹⁻¹¹ In such calculations, force constant matrices (evaluated from the partial second derivatives of the potential) for the *whole* system

(diffusing entity plus substrate) in the minimum energy and saddle point configurations need to be calculated. Consequently, if the system has N atoms, it presents $3N$ modes at the minimum energy configuration and $3N-1$ for the saddle point configuration. With these frequencies, or their densities of states, one calculates the prefactors using the recipe presented in previous publications.^{10,11} While this procedure is feasible when the interaction potentials are of empirical or semi-empirical nature, it becomes quickly formidable, with increasing system size when the interaction is described using density functional theory (DFT). Understandably, calculations of the prefactors based on DFT have been carried out by *totally* or *partially* neglecting the dynamics of the substrate.^{12,13} As a matter of fact, for the studied fcc metals, these approximations do not appear to be drastic, as shown by Ratsch and Scheffler, for the case of Ag adatom diffusion on Ag(111) for which the prefactor changes only by a factor of 2 when the dynamics of the substrate are partially included.¹³ There was thus an informal consensus that for most fcc metals the prefactor for adatom hopping was close to the “standard” value and that the dynamics of the substrate played a minor role in its determination.

In a recent publication, Kong and Lewis,¹⁴ however, claim that the role of the substrate dynamics is crucial for the determination of the prefactor for self-diffusion on the same set of metal surfaces as above. Note that while previous DFT calculations have included the substrate dynamics partially, in one previous study⁹ and see references therein, calculations based on semi-empirical potentials have incorporated the *full* vibrational dynamics of the substrate in calculating all contributions to the system vibrational entropy. Note also that in previous publications^{10,11} while only local contribution to the system vibrational entropy was emphasized, calculations nevertheless included full substrate dynamics. We would like to mention that in a recent study¹⁵ of both adatom and dimer diffusion on the (100) and (110) surfaces of Ag and Cu, using interaction potentials based on the embedded atom method¹⁶ (EAM), we also find the prefactor to be “normal.” As we shall see, noticeable cancellations and

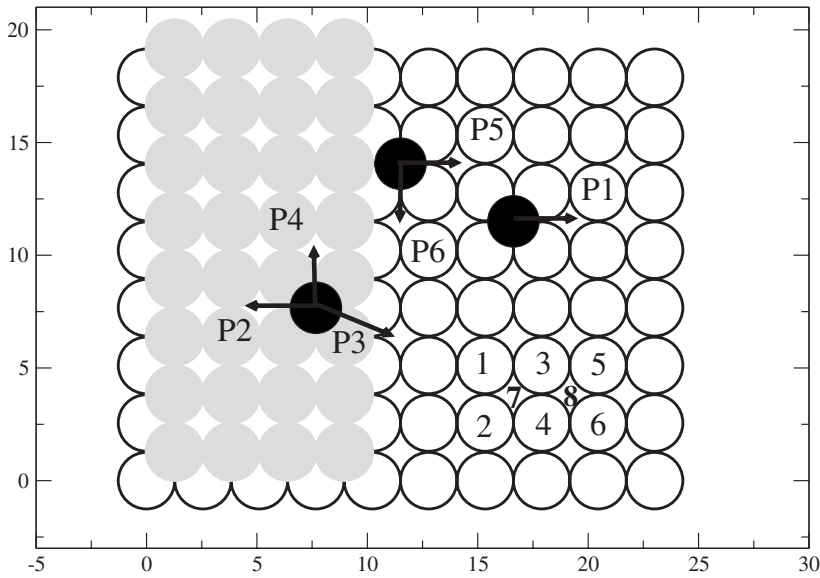


FIG. 1. Investigated processes of adatom diffusion via hopping on fcc(100).

compensations account for the insensitivity of the prefactor to the extended dynamics of the system, for the cases in question.

Two issues now arise. The first is the apparent contradiction between the conclusions reached by Kong and Lewis, and others about the role of the substrate dynamics in determining prefactors for adatom hopping on Cu and Ag surfaces. We realize that there is much confusion in the literature on when and how local approximations are invoked and when extended dynamics play a role. In this work, we isolate the different dynamical contributions and calculate the role of local and extended system geometry in determining the prefactor. The second, and perhaps the more important, is the lack of understanding of the factors that may contribute to a quasi-constant value for the prefactor. To make transparent such contributions, we present, in this paper, a systematic study using both semi-empirical and *ab initio* approaches.

II. THEORETICAL DETAILS

As prototype systems, we consider the case of adatom diffusion via hopping on copper and silver (100) surfaces to demonstrate how local coordination dictates subtle cancellations in contributing to the vibrational free energy that makes the prefactor independent, to a good approximation, of substrate dynamics. Moreover, we show that unless the diffusing entity experiences a dramatic softening and/or stiffening of one or several of its modes, the prefactors lie in the range of 10^{-3} cm²/s, as a result of a compensation resulting from softening of some modes accompanied with stiffening of others. These two effects are general and can be expected to hold for all systems in which coordination is the main player in dictating the variations in vibrational energies and frequencies. To our knowledge, these two microscopic effects have not been reported before. Below, we first present the results for prefactors calculated using the dynamics of the entire system under consideration. Since we use a local ap-

proach to determine vibrational dynamics, a detailed analysis of the contribution of every atom in the system to the dynamics and thermodynamics is possible. We thus separate out the local and the extended contributions and evaluate their relative importance. The local contributions to the prefactor are obtained independently through calculations of vibrational frequencies of the diffusing atom while the substrate is held fixed, as these can be used in the Vineyard equation.²

In Fig. 1, we describe the diffusion processes involving hopping of an adatom from one fcc hollow site to the next on a terrace and near a step edge of a fcc(100) surface. Arrows are used to show the direction along which the adatom performs the diffusion process with the corresponding label. The process labeled P1 corresponds to a hop on a (100) terrace, while processes P2, P3, and P4 are associated, respectively, with an adatom originally on the upper terrace and at the step edge performing (i) a jump away from the step edge, (ii) a descent from the step, and (iii) diffusion along the step. Finally, processes P5 and P6 correspond, respectively, to diffusion on the lower terrace away from and along the step edge, as shown in the figure.

In the semi-empirical approach, the energetics and dynamics of the system (Cu or Ag) are calculated using EAM potentials¹⁶ based on two functionals: one provided by Foiles, Baskes, and Daw (FBD)¹⁷ and the other by Voter and Chen (VC).¹⁸ Total energy electronic structure calculations are also performed using DFT,¹⁹ as implemented in the computational code Vienna ab initio simulation package (VASP).²⁰ The generalized gradient approximation (GGA-PW91) is used to describe the exchange correlation functional.²¹ For calculations using semi-empirical potentials, the system consists of a slab consisting of 14 layers, each containing 64 atoms (8×8) on top of which a 24 atom stripe (3×8) is added for the calculations involving a step. We relax the whole system except the last two layers and fix a few atoms in the stripe to prevent it from sliding during the saddle point search. To obtain relaxed configurations, a standard conjugate gradient method is used for minimizing the total energy of the system.²²

TABLE I. Vibrational free energy contributions per Cu atom (adatom and the first nearest neighbors) at two different configurations of the system.

Atom	Vibrational free energy (meV)	Vibrational free energy (meV)	Vibrational free energy (meV)	Vibrational free energy (meV)
	(Hollow site) 300 K	(Saddle point) 300 K	(Hollow site) 600 K	(Saddle point) 600 K
Adatom	-52	-18	-214	-111
Atoms 1 and 2	-35	-40	-180	-189
Atoms 3 and 4	-35	-26	-180	-163
Atoms 5 and 6	-40	-40	-189	-189
Atom 7	-23	-20	-156	-150
Atom 8	-20	-20	-150	-150

For DFT calculations of bulk systems, energy cutoffs of 234 eV (for Cu) and 181 eV (for Ag) for the plane waves and a $10 \times 10 \times 10$ Monkhorst-Pack k -point sampling of the Brillion zone are used, yielding lattice constants of 3.645 and 4.168 Å for copper and silver, respectively. For flat surface calculations, a $7 \times 7 \times 1$ k -point mesh is used with a unit cell consisting of five layers with four (2×2) atoms per layer. For stepped surfaces, we used a unit cell consisting of four layers with 15 (5×3) atoms per layer, and a stripe consisting of 9 (3×3) atoms and the corresponding k -point mesh is $2 \times 3 \times 1$. In all surface calculations, a vacuum of 12–14 Å is used to separate the slabs. The atoms in the bottom layer of the slab are held fixed during relaxations to prevent a global shift of the slab during the saddle point search.

For complete inclusion of the dynamics of the system, we use a real space Green's function method,^{23,24} which has been described extensively in previous publications.^{9–11} In this method, the vibrational densities of states (VDOSs) for any atom in the system are explicitly evaluated. With these VDOSs in hand, one can calculate all vibrational thermodynamics, and consequently prefactors, within the transition state theory (TST)^{1,2} and the harmonic approximation of the lattice dynamics, using the equation below:

$$D_0(T) = \frac{k_B T n d^2}{h 2\alpha} \exp\left(\frac{-\Delta F_{vib}}{k_B T}\right), \quad (1)$$

where n is the number of equivalent jumps, d and α are jump distance and dimensionality of the motion, respectively. Note that the TST is an approximation based on the assumption that a recrossing at the dividing surface is forbidden (for a detailed discussion on TST, see Ref. 25).

The critical factor in the determination of prefactors is the change in the vibrational free energy ΔF_{vib} , which consists of contributions from all localities of the system. For the discussion here, we divide our system in three parts: the adatom, the atoms labeled 1–8 (Fig. 1) (hereafter, we will drop the word “labeled”), and the rest (atoms 9– N , with $N+1$ being the total number of atoms in the system). Note that by symmetry, atoms 1 and 2, 3 and 4, and 5 and 6 are

equivalent, and hence are grouped in Table I. The total vibrational free energy of the system can hence be written as

$$F_{vib} = F_{vib}^{adatom} + \sum_{i=1}^8 F_{vib}^i + \sum_{j=9}^N F_{vib}^j. \quad (2)$$

III. RESULTS AND DISCUSSION

In Table I, we present the calculated values of F_{vib}^{adatom} and F_{vib}^i , where $i \in [1, 8]$ for the two configurations of Cu adatom (hollow site and saddle point) on Cu(100) for temperatures of 300 and 600 K, using EAM-FBD potential. Analysis of the local vibrational free energy shows that F_{vib}^j for all other atoms where j between 9 and N is independent of whether the adatom is at the hollow site or at the saddle point just as for atom 8 in Table I. Consequently, these atoms do not contribute to ΔF_{vib} and the prefactor. This observation leads to the conclusion that the presence of the adatom affects only locally the vibrational dynamics of the system. The same conclusion has been drawn for vicinal surfaces for which the vibrational dynamics of atoms away from the step were found to be unaffected by the presence of the step.²⁶ We can thus safely conclude that only the neighbors of the diffusing atom contribute to the evaluation of the prefactor, in the systems under consideration.

We now proceed to a detailed analysis of the vibrational free energy of the adatom and its neighbors labeled 1–8 (Table I) for the case of Cu adatom hopping on Cu(100). Clearly, the adatom itself has the largest contribution to the vibrational free energy difference: +34 and +103 meV at 300 and 600 K, respectively. This is followed by atoms 3 and 4 with changes (for each atom) of +9 and +17 meV at 300 and 600 K, respectively. For atoms 1 and 2, these changes are –5 and –9 meV for the two temperatures (note the negative sign for these two atoms). The second layer atom 7 is less affected with changes of +3 and +6 meV for the two temperatures. Finally, the change in the vibrational free energy for atoms 5, 6, and 8 is less than 1 meV. The net change in the vibrational free energy is 45 meV when calculated globally (using the whole system) and 34 meV when using the

dynamics of only the adatom, at 300 K. These values are 125 and 103 meV at 600 K for global and local calculations, respectively. Note that the 103 meV found in this case is very close to that found by Kurpick, Kara, and Rahman (120 meV) who used only the local contribution of the adatom.¹⁰ It is hence obvious from these values that the adatom is the main contributor to the change in the vibrational free energy and hence the prefactor. This is mainly due to the fact that the contribution of atoms 1 and 2 (-10 meV at 300 K) counters that of atoms 3 and 4 ($+18$ meV at 300 K), resulting in a net change that is marginally dependent on the substrate dynamics. To compare our results with those reported by Kong and Lewis, we note that at 600 K, the contribution of the substrate to the change in the vibrational free energy is only 17% in our case as opposed to -200% found by Kong and Lewis¹⁴ (21.00 meV global as opposed to 61.17 meV local). Note that in our case, the contribution of the substrate dynamics to the change of the vibrational free energy is *positive*, while that reported by Kong and Laurent¹⁴ is *negative*. Consequently, in our calculations when the dynamics of the substrate are included, the prefactor decreases slightly in agreement with the findings of Ratch and Scheffler¹³ where as in the case of prefactors reported by Kong and Lewis, the prefactor *always* increases when full dynamics of the system are included in the calculations.¹⁴

Since the compensation effect found above involves mainly atoms 1–4, we present here a physical explanation of the possible origin of these contributions. First, let us analyze the case of atoms 1 and 2 in the two configurations of the adatom. When the adatom is at the hollow site (on top of 7), atoms 1 and 2 are neighbors of the adatom. Since these two atoms are originally from the (100) surface with coordination 8, the presence of the adatom increases their coordination to 9 and their contribution to the vibrational free energy is -35 meV (each), at 300 K, in good agreement with the published value of -33 meV for Cu(111) on which surface atoms have coordination 9.²⁷ When the adatom is placed at the saddle point (on the bridge site between atoms 3 and 4), the coordination of atoms 1 and 2 is back to its surface value which is 8, and for this configuration, from Table I, their contribution is -40 meV (each), again in agreement with previously published value of -39 meV for atoms on Cu(100) at 300 K.²⁷ This change of coordination from 9 to 8 is responsible for a negative contribution to the vibrational free energy. Now let us turn to the case of atoms 3 and 4 for which, using the same arguments, the coordination is 9 when the adatom is at the hollow site, with a contribution of -35 meV (each) at 300 K. When the adatom is placed at the bridge site, its coordination now is only two which forces its distance to atoms 3 and 4 to shrink (the bond length drops from 2.417 to 2.309 Å), causing an increase in the vibrational free energy of atoms 3 and 4 that reaches the value of -26 meV. This behavior is consistent with our previous published conclusions on the behavior of the local vibrational free energy versus coordination and bond lengths.²⁸

Having demonstrated that the substrate dynamics may be neglected for evaluating prefactors for Cu adatom diffusion via hopping on Cu(100), we can simplify our approach and get further insights into adatom diffusion by focusing only

on its vibrational frequencies. In other words, we will use the frozen phonon method in which we calculate the frequencies of the normal modes (of the adatom): three modes at the minimum energy configuration and two modes at the saddle point. To determine the frequencies of these modes from EAM-FBD and EAM-VC, local force constants are obtained from the calculated total energy of the system. For example, for the adatom diffusion along the x direction, we start with the adatom in the fcc hollow site configuration and perform three sets of calculations corresponding to the adatom being placed between -0.2 and $+0.2$ Å around the equilibrium position and along the x , y , or z direction, with an increment of 0.02 Å. At the saddle point (taking the diffusion path to be along the x axis), only two sets of calculations are performed along the y and z directions, with the same increment. Each set of calculations provides the energy of the system versus position around the equilibrium and/or saddle which was then fitted by a quadratic function yielding the force constant associated with the normal mode along that direction. The same procedure has been adopted when using DFT calculations except that here the number of points along a given direction is reduced to 5 (a check using seven points did not introduce any change in the frequencies). To introduce substrate vibrational contribution (in the case of DFT calculations), we added the frequencies of the nearest neighbors of the adatom. Note that in a previous publication, we have already presented the results for prefactors for the above mechanisms on Cu(100) and Cu(110) using EAM-FBD potentials and with the inclusion of the vibrational dynamics of the whole system.⁹

A comparison of the frequencies of the normal modes of the adatom (Cu or Ag) on Cu(100) and Ag(100) obtained from either of the EAM functionals and DFT shows interesting trends as may be noted from the plots in Fig. 2, in which differences in the calculated frequencies are noted by their deviation from the diagonal. From Fig. 2(a) (the case of Cu), one notes that the force field around the adatom as described by VC functional is stiffer than that described by FBD functional. However, this is not true for Ag [see Fig. 2(b)] for which we find no systematic trend for either functional to yield stiffer force field. The same observation holds when comparing DFT-GGA and FBD [Fig. 2(c)] for which we again find a tendency for FBD to yield a softer force field than DFT-GGA (with the exception of the case of saddle point for process P6). For Ag [Fig. 2(d)], the tendency for DFT-GGA to yield a stiffer force field is less pronounced than the case of Cu. One general observation is that differences in the calculated frequencies using the different potentials do not exceed 0.7 THz, for all cases studied here. Since exact values of the calculated frequencies may be of the interest to the reader, we have summarized them in Appendix A.

When substrate dynamics are neglected, the calculations of the prefactor follows trivially from the Eq. (1), using the adatom normal mode frequencies to calculate the difference in the vibrational entropy. Such prefactors for several diffusion processes of Cu adatom on Cu(100) and Ag adatom on Ag(100) using EAM-FBD, EAM-VC, and DFT-GGA are presented in Tables IV and V in Appendix B, respectively.

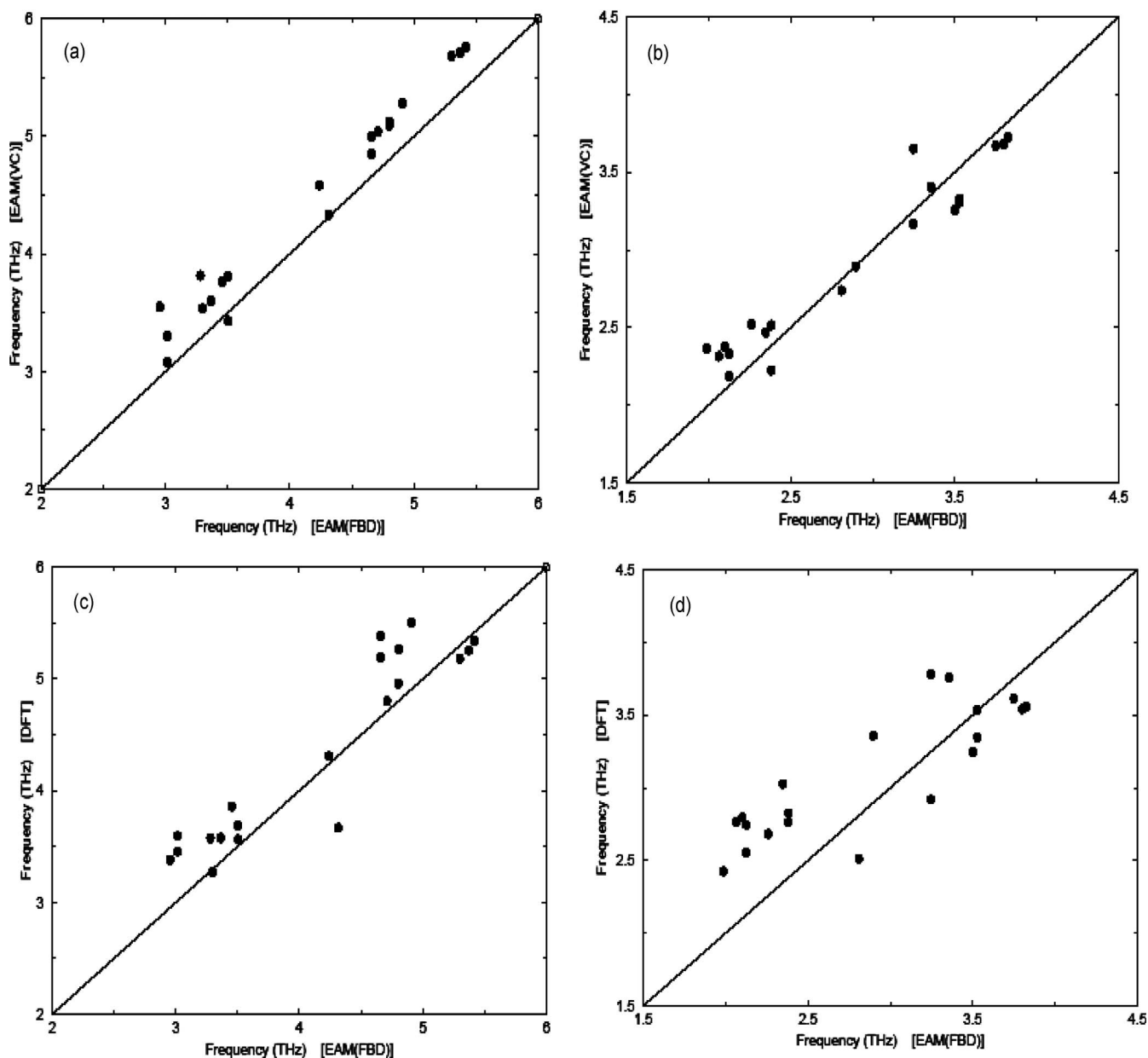


FIG. 2. Comparison of the calculated frequencies for adatom diffusion processes shown in Fig. 1. (a) For Cu(100) using EAM-FBD and EAM-VC; (b) for Ag(100) using EAM-FBD and EAM-VC; (c) for Cu(100) using EAM-FBD and DFT-GGA; (d) for Ag(100) using EAM-FBD and DFT-GG.

The prefactor values that are obtained from DFT (when dynamics of neighboring substrate atoms are included) are also presented in these tables. From these tables, we note that the prefactors do not deviate by more than a factor of 2 from the so-called normal value of “ 10^{-3} cm²/s,” in agreement with previous results.^{3–11,29} Since the temperatures chosen here are close to or higher than the Debye temperature of the solid, as expected^{9–11} temperature has almost no effect on prefactors. It is interesting to point out that even when we include the full substrate dynamics, as we did in our previous publication⁹ for Cu adatom diffusion on Cu(100) and Cu(110), the prefactors also lie within a factor of 2 as compared to those presented here, with the exception of the case of process P1 for which the factor is 2.89.

Another observation that can be deduced from the tables is that, even if the frequencies of the modes calculated from different potentials showed differences, these are washed out in the thermodynamic functions because of a subtle but systematic compensation effect. Indeed, in general, modes with polarization parallel to the surface have their frequencies soften when moving from the hollow site to the saddle point, while the frequencies of modes with polarization perpendicular to the surface experience stiffening. This again can be rationalized in terms of coordination of the adatom. Indeed, at equilibrium [let us say on fcc(100) surface], the adatom coordination is 4 and it drops to 2 when the atom is at the bridge (saddle) point. The loss of (in-plane) neighbors causes the softening of the in-plane (parallel) mode. On the other

TABLE II. Ratios of the frequencies of the adatom parallel and perpendicular to the surface for each process (values in the parenthesis are for silver).

Processes	EAM-FBD		EAM-VC		DFT-GGA	
	r_{\parallel}	r_{\perp}	r_{\parallel}	r_{\perp}	r_{\parallel}	r_{\perp}
P1 Hopping on flat	1.11 (1.14)	0.89 (0.93)	1.08 (1.07)	0.89 (0.89)	1.06 (1.10)	0.93 (0.90)
P2 Diffusion <i>away</i> from step on the upper terrace	1.04 (1.12)	0.89 (0.93)	1.06 (1.04)	0.90 (0.90)	1.03 (1.08)	0.94 (0.95)
P3 Diffusion rolling <i>over</i> step	1.10 (1.18)	1.00 (1.01)	1.11 (1.13)	1.01 (1.00)	1.04 (1.03)	0.94 (0.95)
P4 Diffusion <i>along</i> the step on the upper terrace	1.06 (1.16)	0.86 (0.92)	1.08 (1.08)	0.89 (0.90)	1.13 (1.02)	0.93 (0.94)
P5 Diffusion <i>away</i> from step on the lower terrace	0.92 (1.02)	0.88 (0.86)	1.07 (0.94)	0.97 (0.87)	0.96 (0.94)	0.96 (0.77)
P6 Diffusion <i>along</i> step on the lower terrace	0.98 (1.03)	0.95 (0.97)	1.06 (1.05)	0.92 (0.93)	1.17 (1.33)	0.94 (0.78)

hand, at the saddle point, the coordination being very low and due to the bond-length/bond-order correlation, the relaxation is such that the adatom bond to the two surface atoms shortens drastically (the shortening involves mostly the component perpendicular to the surface), resulting in a stiffening of the perpendicular mode. This is a general argument that can be transferred to other surface geometries and we are in the process of testing the validity of these arguments on (110) and (111) surfaces. To quantify this observation, let us use the Vineyard equation² for the prefactor:

$$D_0 \propto \frac{\nu_1^h \nu_2^h \nu_3^h}{\nu_2^s \nu_3^s}, \quad (3)$$

where ν_1^h , ν_2^h , and ν_3^h are the frequencies of the three normal modes when the adatom is in the hollow site and ν_2^s and ν_3^s are those corresponding to the saddle point (here we assume that the diffusion path is along direction “1”). Note that in the classical limit, Eq. (1) reduces to Eq. (3). We introduce the ratio $r_{\parallel} = \nu_2^h / \nu_2^s$, $r_{\perp} = \nu_3^h / \nu_3^s$, assuming that direction “2” is parallel to the surface (either x or y , depending on the process) and direction “3” is perpendicular to the surface (z). In Table II, we present these ratios of the frequencies for the adatom on Cu and Ag surfaces for each diffusion process. We find that while these ratios never exceed 1.4 nor go below 0.7, in general, r_{\parallel} is larger than 1 (the mode parallel to the surface goes soft) while r_{\perp} is less than 1 (the mode goes stiff). Since the prefactor is proportional to the product of these two ratios, the net effect of the coupled softening and stiffening of the modes is to keep the prefactor almost constant. We expect this compensation effect to be general, at least for hopping processes, and present it as the rationale for

the general tendency of the prefactor to stay close to the “normal” value of 10^{-3} cm²/s.

IV. CONCLUSIONS

In conclusion, we have determined the pre-exponential factors of several processes for adatom diffusion via hopping on Ag(100) and Cu (100) including and excluding the full dynamics of the substrate. Two types of semi-empirical potentials and a first principles approach are used. We find that including the substrate dynamics in the determination of pre-exponential factors does not introduce pronounced effects (a factor less than 2 is, in general, observed) for adatom diffusion via hopping on flat and stepped surfaces of copper and silver, regardless of the method for determining interatomic interaction. Compensation effects in the vibrational frequencies of the diffusing entity and cancellations in the change of the vibrational free energy are responsible for the quasi-constant value around 10^{-3} cm²/s reported frequently in the literature.

The arguments used here to rationalize the quasi-constant value of the prefactor are based on coordination and one would need to test its validity neither for more complex situations at which the diffusion is not single atom nor via hopping, like in the case of an exchange mechanism. We are extending our work to the exchange mechanism, multi-atom (islands) diffusion as well as diffusion on (110) and (111) surfaces.

ACKNOWLEDGMENTS

This work was supported by NSF-ITR Grant No. 0428826 and computer resources were provided by NCSA under Grant No. TG-DMR070005T.

APPENDIX A: CALCULATED FREQUENCIES OF THE NORMAL MODES OF ADATOM (TABLE III)

TABLE III. The frequencies of the adatom on Cu(100) and Ag(100) (in parantheses) for diffusion processes in Fig. 1 using EAM-FBD, EAM-VC, and DFT-GGA (without substrate contribution).

Systems	Direction of the mode	Frequencies EAM-FBD (THz)	Frequencies EAM-VC (THz)	Frequencies DFT-GGA (THz)
P1 Hopping on flat	(Hollow)			
	<i>x, y</i>	3.28 (2.26)	3.82 (2.52)	3.58 (2.68)
	<i>z</i>	4.71 (3.50)	5.04 (3.26)	4.80 (3.24)
	(Saddle)			
	<i>y</i>	2.95 (1.99)	3.55 (2.36)	3.38 (2.43)
	<i>z</i>	5.30 (3.75)	5.68 (3.67)	5.18 (3.62)
P2 Diffusion <i>away</i> from the step on the upper terrace	(Hollow)			
	<i>x</i>	3.46 (2.35)	3.77 (2.47)	3.86 (3.03)
	<i>y</i>	3.50 (2.38)	3.81 (2.52)	3.69 (2.83)
	<i>z</i>	4.80 (3.53)	5.12 (3.33)	4.96 (3.35)
	(Saddle)			
	<i>y</i>	3.37 (2.10)	3.59 (2.38)	3.58 (2.80)
	<i>z</i>	5.37 (3.80)	5.71 (3.68)	5.26 (3.54)
P3 Diffusion rolling <i>over</i> step	(Hollow)			
	<i>x</i>	3.46 (2.35)	3.77 (2.47)	3.86 (3.03)
	<i>y</i>	3.50 (2.38)	3.81 (2.52)	3.69 (2.83)
	<i>z</i>	4.80 (3.53)	5.12 (3.33)	4.96 (3.35)
	(Saddle)			
	<i>y</i>	3.17 (2.02)	3.43 (2.23)	3.56 (2.76)
	<i>z</i>	4.80 (3.50)	5.09 (3.31)	5.27 (3.54)
P4 Diffusion <i>along</i> the step on the upper terrace	(Hollow)			3.86 (3.03)
	<i>x</i>	3.46 (2.35)	3.77 (2.47)	3.69 (2.83)
	<i>y</i>	3.50 (2.38)	3.81 (2.52)	4.96 (3.35)
	<i>z</i>	4.80 (3.53)	5.12 (3.33)	
	(Saddle)			
	<i>y</i>	3.30 (2.07)	3.53 (2.32)	3.27 (2.77)
	<i>z</i>	5.42 (3.83)	5.76 (3.72)	5.34 (3.56)
P5 Diffusion <i>away</i> from the step on the lower terrace	(Hollow)			
	<i>x</i>	4.24 (2.90)	4.59 (2.89)	4.31 (3.36)
	<i>y</i>	3.02 (2.13)	3.30 (2.19)	3.46 (2.55)
	<i>z</i>	4.66 (3.25)	4.85 (3.17)	5.19 (2.92)
	(Saddle)			
	<i>y</i>	3.28 (2.08)	3.08 (2.33)	3.59 (2.75)
	<i>z</i>	5.32 (3.79)	4.99 (3.65)	5.39 (3.78)
P6 Diffusion <i>along</i> the step on the lower terrace	(Hollow)			
	<i>x</i>	4.24 (2.90)	4.59 (2.89)	4.31 (3.36)
	<i>y</i>	3.02 (2.13)	3.30 (2.19)	3.46 (2.55)
	<i>z</i>	4.66 (3.25)	4.85 (3.17)	5.19 (2.92)
	(Saddle)			
	<i>x</i>	4.32 (2.81)	4.33 (2.74)	3.67 (2.51)
	<i>z</i>	4.91 (3.35)	5.29 (3.41)	5.50 (3.76)

APPENDIX B: PRE-EXPONENTIAL FACTORS (PREFACTORS) AND DIFFUSION COEFFICIENTS)
(TABLE IV AND V)

TABLE IV. Prefactors and diffusion coefficients at two different temperatures for adatom diffusion via hopping on flat and stepped surfaces of Cu(100) using DFT-GGA, EAM-FBD, and EAM-VC. Results in { } refers to DFT-GGA (with substrate contribution), [] for DFT-GGA (without substrate contribution), () for EAM-FBD and (()) for EAM-VC calculations (without substrate contribution).

Systems	$D_0(T)$ (cm^2/s) 300 K	$D_0(T)$ (cm^2/s) 600 K	$D(T)$ (cm^2/s) 300 K	$D(T)$ (cm^2/s) 600 K
P1 Hopping on flat	{ 3.00×10^{-3} }	{ 2.95×10^{-3} }	{ 1.72×10^{-12} }	{ 7.06×10^{-8} }
	[2.30×10^{-3}]	[2.28×10^{-3}]	[1.32×10^{-12}]	[5.46×10^{-8}]
	(2.12×10^{-3})	(2.11×10^{-3})	(7.43×10^{-12})	(1.11×10^{-7})
	((2.39×10^{-3}))	((2.37×10^{-3}))	((3.31×10^{-12}))	((8.83×10^{-8}))
P2 Diffusion <i>away</i> from the step on the upper-terrace	{ 1.32×10^{-3} }	{ 1.31×10^{-3} }	{ 1.83×10^{-12} }	{ 4.87×10^{-8} }
	[1.24×10^{-3}]	[1.22×10^{-3}]	[1.72×10^{-12}]	[4.56×10^{-8}]
	(1.05×10^{-3})	(1.04×10^{-3})	(8.61×10^{-12})	(9.47×10^{-8})
	((1.17×10^{-3}))	((1.16×10^{-3}))	((4.27×10^{-12}))	((7.03×10^{-8}))
P3 Diffusion rolling <i>over</i> step	{ 1.24×10^{-3} }	{ 1.22×10^{-3} }	{ 1.14×10^{-14} }	{ 3.72×10^{-9} }
	[1.24×10^{-3}]	[1.23×10^{-3}]	[1.15×10^{-14}]	[3.73×10^{-9}]
	(1.26×10^{-3})	(1.25×10^{-3})	(7.47×10^{-17})	(3.04×10^{-10})
	((1.39×10^{-3}))	((1.37×10^{-3}))	((1.69×10^{-17}))	((1.52×10^{-10}))
P4 Diffusion <i>along</i> the step on the upper terrace	{ 3.80×10^{-3} }	{ 3.75×10^{-3} }	{ 4.03×10^{-12} }	{ 1.22×10^{-7} }
	[2.66×10^{-3}]	[2.64×10^{-3}]	[2.83×10^{-12}]	[8.56×10^{-8}]
	(2.13×10^{-3})	(2.12×10^{-3})	(9.40×10^{-12})	(1.40×10^{-7})
	((2.37×10^{-3}))	((2.35×10^{-3}))	((3.29×10^{-12}))	((8.77×10^{-8}))
P5 Diffusion <i>away</i> from the step on the lower terrace	{ 1.72×10^{-3} }	{ 1.71×10^{-3} }	{ 1.41×10^{-22} }	{ 4.91×10^{-13} }
	[1.32×10^{-3}]	[1.30×10^{-3}]	[1.08×10^{-22}]	[3.73×10^{-13}]
	(1.12×10^{-3})	(1.11×10^{-3})	(7.38×10^{-18})	(9.03×10^{-11})
	((1.59×10^{-3}))	((1.56×10^{-3}))	((6.15×10^{-17}))	((3.07×10^{-10}))
P6 Diffusion <i>along</i> the step on the lower terrace	{ 2.67×10^{-3} }	{ 2.64×10^{-3} }	{ 1.66×10^{-8} }	{ 6.56×10^{-6} }
	[2.53×10^{-3}]	[2.50×10^{-3}]	[1.57×10^{-8}]	[6.23×10^{-6}]
	(1.84×10^{-3})	(1.83×10^{-3})	(6.73×10^{-8})	(1.11×10^{-5})
	((2.11×10^{-3}))	((2.09×10^{-3}))	((4.32×10^{-8}))	((9.48×10^{-6}))

TABLE V. Prefactors and diffusion coefficients at two different temperatures for adatom diffusing on flat and stepped surfaces of Ag(100) using DFT-GGA, EAM-FBD and EAM-VC. Results in { } refers to DFT-GGA (with substrate contribution), [] for DFT-GGA (without substrate contribution), () for EAM-FBD, and (()) for EAM-VC calculations (without substrate contribution).

Systems	$D_0(T)$ (cm^2/s) 300 K	$D_0(T)$ (cm^2/s) 600 K	$D(T)$ (cm^2/s) 300 K	$D(T)$ (cm^2/s) 600 K
P1 Hopping on flat	{ 2.59×10^{-3} }	{ 2.58×10^{-3} }	{ 1.12×10^{-10} }	{ 5.34×10^{-7} }
	[2.25×10^{-3}]	[2.24×10^{-3}]	[9.68×10^{-11}]	[4.65×10^{-7}]
	(1.57×10^{-3})	(1.56×10^{-3})	(5.49×10^{-12})	(9.25×10^{-7})
	((2.02×10^{-3}))	((2.01×10^{-3}))	((1.59×10^{-11}))	((1.79×10^{-7}))
P2 Diffusion <i>away</i> from the step on the upper terrace	{ 1.71×10^{-3} }	{ 1.69×10^{-3} }	{ 1.85×10^{-10} }	{ 5.57×10^{-7} }
	[1.23×10^{-3}]	[1.22×10^{-3}]	[1.33×10^{-10}]	[4.00×10^{-7}]
	(1.05×10^{-3})	(1.04×10^{-3})	(9.59×10^{-12})	(9.98×10^{-8})
	((9.98×10^{-4}))	((9.95×10^{-4}))	((1.35×10^{-11}))	((1.16×10^{-7}))
P3 Diffusion rolling <i>over</i> step	{ 1.65×10^{-3} }	{ 1.64×10^{-3} }	{ 3.28×10^{-11} }	{ 2.30×10^{-7} }
	[1.24×10^{-3}]	[1.23×10^{-3}]	[2.47×10^{-11}]	[1.74×10^{-7}]
	(1.18×10^{-3})	(1.17×10^{-3})	(1.56×10^{-13})	(1.35×10^{-8})
	((1.19×10^{-3}))	((1.18×10^{-3}))	((2.27×10^{-15}))	((1.63×10^{-9}))
P4 Diffusion <i>along</i> the step on the upper terrace	{ 2.85×10^{-3} }	{ 2.83×10^{-3} }	{ 1.27×10^{-10} }	{ 5.97×10^{-7} }
	[2.47×10^{-3}]	[2.45×10^{-3}]	[1.10×10^{-10}]	[5.18×10^{-7}]
	(2.11×10^{-3})	(2.10×10^{-3})	(1.94×10^{-11})	(2.02×10^{-7})
	((2.03×10^{-3}))	((2.02×10^{-3}))	((1.72×10^{-11}))	((1.86×10^{-7}))
P5 Diffusion <i>away</i> from the step on the lower terrace	{ 1.05×10^{-3} }	{ 1.04×10^{-3} }	{ 1.31×10^{-14} }	{ 3.72×10^{-9} }
	[1.02×10^{-3}]	[1.01×10^{-3}]	[1.28×10^{-14}]	[3.60×10^{-9}]
	(1.07×10^{-3})	(1.06×10^{-3})	(2.99×10^{-15})	(1.78×10^{-9})
	((9.95×10^{-4}))	((9.92×10^{-4}))	((1.87×10^{-16}))	((4.30×10^{-10}))
P6 Diffusion <i>along</i> the step on the lower terrace	{ 2.12×10^{-3} }	{ 2.11×10^{-3} }	{ 2.87×10^{-7} }	{ 2.46×10^{-5} }
	[2.24×10^{-3}]	[2.23×10^{-3}]	[3.04×10^{-7}]	[2.60×10^{-5}]
	(1.79×10^{-3})	(1.78×10^{-3})	(1.17×10^{-7})	(1.44×10^{-5})
	((1.82×10^{-3}))	((1.81×10^{-3}))	((8.05×10^{-8}))	((1.20×10^{-5}))

¹C. Wert and C. Zener, Phys. Rev. **76**, 1169 (1949).

²G. H. Vineyard, J. Phys. Chem. Solids **3**, 121 (1957).

³G. Ehrlich, in *Surface Diffusion: Atomistic and Collective Processes*, edited by Michael C. Tringides (Plenum, New York, 1997), p. 23; G. L. Kellogg, Surf. Sci. Rep. **21**, 1 (1994).

⁴S. G. Wang and G. Ehrlich, Surf. Sci. **206**, 451 (1988).

⁵K. A. Fichthorn and M. Scheffler, Phys. Rev. Lett. **84**, 5371 (2000).

⁶A. Bogicevic, S. Ovesson, P. Hyltdgaard, B. I. Lundqvist, H. Brune, and D. R. Jennison, Phys. Rev. Lett. **85**, 1910 (2000).

⁷G. L. Kellogg and P. J. Fiebelman, Phys. Rev. Lett. **64**, 3143 (1990).

⁸G. L. Kellogg, A. F. Wright, and M. S. Daw, J. Vac. Sci. Technol.

A **9**, 1757 (1991).

⁹H. Yildirim, A. Kara, S. Durukanoglu, and T. S. Rahman, Surf. Sci. **600**, 484 (2006) and references therein.

¹⁰U. Kurpick, A. Kara, and T. S. Rahman, Phys. Rev. Lett. **78**, 1086 (1997); U. Kurpick and T. S. Rahman, Surf. Sci. **427-428**, 15 (1999).

¹¹U. Kurpick and T. S. Rahman, Phys. Rev. B **57**, 2482 (1998); U. Kurpick, *ibid.* **64**, 075418 (2001); S. Durukanoglu, A. Kara, and T. S. Rahman, Surf. Sci. **587**, 128 (2005).

¹²L. Xu, G. Henkelman, C. T. Campbell, and H. Jonsson, Surf. Sci. **600**, 1351 (2006).

¹³C. Ratsch and M. Scheffler, Phys. Rev. B **58**, 13163 (1998).

¹⁴L. T. Kong and Laurent J. Lewis, Phys. Rev. B **74**, 073412

- (2006).
- ¹⁵H. Yildirim, A. Kara, and T. S. Rahman (unpublished).
- ¹⁶M. S. Daw, S. M. Foiles, and M. I. Baskes, *Mater. Sci. Rep.* **9**, 251 (1993).
- ¹⁷S. M. Foiles, M. I. Baskes, and M. S. Daw, *Phys. Rev. B* **33**, 7983 (1986); M. S. Daw, S. M. Foiles, and M. I. Baskes, *Mater. Sci. Rep.* **9**, 251 (1993).
- ¹⁸A. F. Voter and S. P. Chen, in *Characterization of Defects in Materials*, edited by R. W. Siegel, J. R. Weertman, and R. Sinclair, MRS Symposia Proceedings No. 82 (Materials Research Society, Pittsburgh, 1986), p. 175.
- ¹⁹P. Hohenberg and W. Kohn, *Phys. Rev.* **136**, B864 (1964); W. Kohn and L. J. Sham, *ibid.* **140**, A1133 (1965).
- ²⁰G. Kresse and J. Hafner, *Phys. Rev. B* **47**, 558 (1993); **49**, 14251 (1994); G. Kresse and J. Furthmüller, *Comput. Mater. Sci.* **6**, 15 (1996); *Phys. Rev. B* **54**, 11169 (1996).
- ²¹J. P. Perdew and Y. Wang, *Phys. Rev. B* **45**, 13244 (1992).
- ²²W. Press, S. Teukolsky, W. Vetterling, and B. Flannery, *Numerical Recipes in Fortran* (Cambridge University Press, Cambridge, 1992).
- ²³S. Y. Wu, J. Cocks, and C. S. Jayanthi, *Phys. Rev. B* **49**, 7957 (1994).
- ²⁴A. Kara, C. S. Jayanthi, S. Y. Wu, and F. Ercolessi, *Phys. Rev. Lett.* **72**, 2223 (1994).
- ²⁵T. Ala-Nissila, R. Ferrando, and S. C. Ying, *Adv. Phys.* **51**, 949 (2002).
- ²⁶A. Kara and T. S. Rahman, *Surf. Sci.* **502-503**, 449 (2002).
- ²⁷S. Durukanoglu, A. Kara, and T. S. Rahman, *Phys. Rev. B* **67**, 235405 (2003).
- ²⁸A. Kara and T. S. Rahman, *Surf. Sci. Rep.* **56**, 159 (2004).
- ²⁹C. L. Liu, J. M. Cohen, J. B. Adams, A. F. Voter, *Surf. Sci.* **253**, 334 (1991).